Phosphorus Heterocycles

Deutsche Ausgabe: DOI: 10.1002/ange.201500229
Internationale Ausgabe: DOI: 10.1002/anie.201500229

Environment-Sensitive Fluorescent Probe: A Benzophosphole Oxide with an Electron-Donating Substituent**

Eriko Yamaguchi, Chenguang Wang, Aiko Fukazawa, Masayasu Taki, Yoshikatsu Sato, Taeko Sasaki, Minako Ueda, Narie Sasaki, Tetsuya Higashiyama,* and Shigehiro Yamaguchi**

Abstract: *Electron-donating aryl groups were attached to electron-accepting benzophosphole skeletons. Among several derivatives thus prepared, one benzophosphole oxide was particularly interesting, as it retained high fluorescence quantum yields even in polar and protic solvents. This phosphole-based compound exhibited a drastic color change of its fluorescence spectrum as a function of the solvent polarity, while the absorption spectra remained virtually unchanged. Capitalizing on these features, this phosphole-based compound was used to stain adipocytes, in which the polarity of subcellular compartments could then be discriminated on the basis of the color change of the fluorescence emission.*

Phosphole, a heavier phosphorus analogue of pyrrole, is an attractive building block for π-conjugated materials.[1] Whereas pyrrole is aromatic and has electron-donating properties, phosphole is nonaromatic and exhibits an electron-accepting character.[1b,2] Relative to pyrrole, the lone-pair electrons of the pyramidalized phosphorus atom in the phosphole conjugate to a lesser extent with the π-system. Instead, effective orbital interaction occurs between the π* orbital of a butadiene moiety and the σ* orbital of an exocyclic σ bond on the phosphorus atom, thus resulting in a decreased LUMO level. The electron-accepting properties of phosphole can be further increased by facile transformations into phosphine oxides, phosphine sulfides, phosphonium salts, and metal complexes. Among these, especially the phosphine oxide and sulfide derivatives exhibit desirably high thermal and chemical stability. Taking advantage of these features, phosphole-based materials have been widely applied in organic electronics,[1g,h] including organic light-emitting diodes[3,4] and photovoltaics.[5] However, biological applications have not yet been explored exhaustively. In this context, we would like to disclose here the successful development of highly fluorescent phosphole derivatives, and demonstrate their potential as fluorescent bioimaging probes.

The combination of an electron-accepting π-skeleton with an electron-donating moiety represents a rational design approach for producing environment-sensitive fluorescent molecules.[6] Following this avenue, we have now designed the

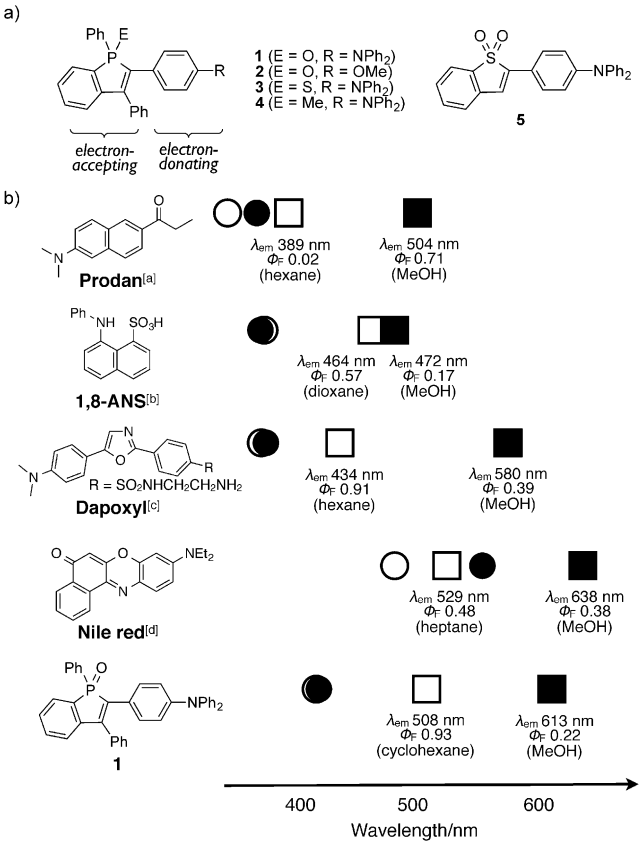

Figure 1. a) Chemical structures of the benzophosphole derivatives **1**–**4** and benzothiophene dioxide congener **5**. b) Comparison of representative environment-sensitive fluorescent probes, whereby circles and squares represent the maxima of absorption and emission, respectively. Empty and filled symbols denote wavelengths in nonpolar and polar solvents, respectively. [a] Reference [8b]; [b] Reference [9b,c]; [c] Reference [10]; [d] Reference [11b].

[*] E. Yamaguchi, Prof. Dr. A. Fukazawa, Prof. Dr. S. Yamaguchi
Department of Chemistry, Graduate School of Science
Nagoya University
Furo, Chikusa, Nagoya 464-8602 (Japan)
E-mail: aiko@chem.nagoya-u.ac.jp
yamaguchi@chem.naogya-u.ac.jp
T. Sasaki, Prof. Dr. N. Sasaki, Prof. Dr. T. Higashiyama
Division of Biological Science, Graduate School of Science
Nagoya University, Furo, Chikusa, Nagoya 464-8602 (Japan)
C. Wang, Prof. Dr. M. Taki, Dr. Y. Sato, Dr. M. Ueda,
Prof. Dr. T. Higashiyama, Prof. Dr. S. Yamaguchi
Institute of Transformative Bio-Molecules (WPI-ITbM)
Nagoya University, Furo, Chikusa, Nagoya 464-8602 (Japan)
E-mail: higashi@bio.nagoya-u.ac.jp

[**] This work was supported by JST, CREST (S.Y.), a Grant-in-Aid for Scientific Research on Innovative Areas "Organic Synthesis based on Reaction Integration" (no. 2105) from MEXT (Japan) (A.F.), and the Japan Advanced Plant Science Network. E.Y. thanks the JSPS for a Research Fellowship for Young Scientists. ITbM is supported by the World Premier International Research Center (WPI) Initiative, Japan.

Supporting information for this article is available on the WWW under http://dx.doi.org/10.1002/anie.201500229.

environment-sensitive fluorescent molecule **1** by combining an electron-accepting benzophosphole oxide with an electron-donating triphenylamine substituent (Figure 1a). Environment-sensitive fluorescent probes are particularly important for the visualization of polarity changes associated with cellular events,[7] and the general requirements for such probes are: 1) high fluorescence quantum yields (Φ_F) irrespective of the solvent polarity, 2) large Stokes shifts to avoid autofluorescence interference, and 3) drastic color change of the fluorescence emission as a function of the solvent polarity. Several previously reported fluorophores, such as prodan,[8] 1,8-ANS,[9] dapoxyl,[10] and Nile red,[11] are known to satisfy these requisites. However, in comparison to these, **1** offers the following additional advantages: 1) compatibility with 405 nm light-emitting diode lasers, which are frequently used for excitation in fluorescence microscopy, and 2) bathochromically shifted reddish fluorescence emission as a result of excitation with such a 405 nm laser (Figure 1b). Herein, we discuss the key structural requisites necessary for our new fluorophore to exhibit its characteristic fluorescence properties, and we also demonstrate its application in cell imaging.

An important advantage of benzophosphole oxide as an electron-accepting building block is the facile synthetic access to its skeleton. Recently, several new reactions have been developed for the synthesis of benzophospholes.[12] Our contributions to this area include a versatile synthesis for benzophospholes based on the intramolecular *trans*-halophosphanylation of *o*-phosphanylphenylacetylenes,[13,14] which afforded a series of donor–acceptor-type benzophospholes. Thus, starting from the (*o*-bromophenyl)(*p*-substituted phenyl)acetylene precursors **6**, a lithiation with two equivalents of *t*BuLi, followed by treatment with PhP(NEt$_2$)Cl generated the corresponding *o*-aminophosphanyl-substituted intermediates (Scheme 1). Without isolation, a subsequent treatment with PBr_3 resulted in the halogenation of the phosphorus moiety, followed by an intramolecular cyclization by *trans*-halophosphanylation. This convenient one-pot procedure furnished the 3-bromobenzo[*b*]phosphole oxides **7**, bearing electron-donating aryl groups at the 2-position, in moderate to good yields. An ensuing Suzuki–Miyaura cross-coupling reaction of **7** with phenylboronic acid under standard reaction conditions afforded the derivatives **1** and **2** in good yields. The compound **1** was further transformed into the corresponding phosphole sulfide **3** by treatment with Lawesson's reagent. An analogous phosphonium derivative **4** was also prepared by the reduction of **1** with $HSiCl_3$, and subsequent treatment with methyl triflate. The structures of these compounds were assigned unequivocally based on the results from NMR spectroscopy and mass spectrometry measurements.

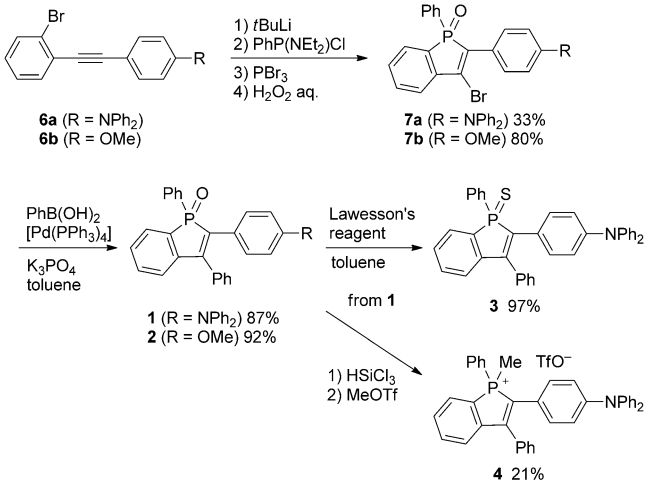

Scheme 1. Synthesis of the donor-substituted benzophosphole derivatives **1**–**4**. Tf = trifluoromethanesulfonyl.

The *p*-(diphenylamino)phenyl-substituted benzophosphole oxide **1** exhibited excellent fluorescent properties (Table 1). In toluene, the absorption maximum of **1** was observed at $\lambda_{abs} = 415$ nm, while an intense fluorescence band with a fluorescence quantum yield (Φ_F) of 0.94 was recorded at $\lambda_{em} = 528$ nm. With increasing solvent polarity, the absorption spectra showed only subtle changes ($\lambda_{abs} = 403$–420 nm), whereas the fluorescence bands were shifted significantly in a bathochromic direction (DMSO: 601 nm; EtOH: 593 nm). Most notably, **1** preserves high fluorescence quantum yields in polar (DMSO: $\Phi_F = 0.64$) and protic solvents (EtOH: $\Phi_F = 0.58$) despite the corresponding large Stokes shifts (DMSO: 7630 cm^{-1}; EtOH: 7120 cm^{-1}). The fact that a brightness of the fluorescence, denoted by the product of molar extinction coefficient (ε) and Φ_F,[15] of about 10^4 was attained even in ethanol, thus suggests potential applications for this compound as a fluorescent probe.

Table 1: Photophysical properties of **1**–**5** in various solvents.

Cmpd	Solvents	λ_{abs} [nm][a]	ε [10^4 M^{-1} cm^{-1}]	λ_{em} [nm]	Φ_F[b]	$\varepsilon \times \Phi_F$ [10^4 M^{-1} cm^{-1}]
1	toluene	415	1.87	528	0.94	1.8
	$CHCl_3$	420	1.74	553	0.94	1.6
	CH_2Cl_2	415	1.73	565	0.90	1.6
	acetone	403	1.73	575	0.84	1.5
	ethanol	417	1.60	593	0.58	0.9
	DMSO	412	1.66	601	0.64	1.1
2	toluene	364	1.03	471	0.74	0.8
	DMSO	364	0.94	490	0.69	0.7
3	toluene	412	1.58	526	0.87	1.4
	DMSO	411	1.28	608	0.61	0.8
4	toluene	448	1.34	672	0.20	0.3
	DMSO	440	1.23	702	0.02	0.02
5	toluene	419	2.56	507	0.92	2.4
	DMSO	418	2.29	628	0.06	0.1

[a] Longest wavelength absorption maximum. [b] Absolute fluorescence quantum yields determined with a calibrated integrating sphere system (errors < 3%).

A comparison of **1** with related compounds, including the anisyl-substituted **2**, containing a weaker electron-donating substituent, as well as with the electron-accepting benzophosphole sulfide **3**, phosphonium salt **4**, and thiophene dioxide congener **5**, demonstrates that the well-balanced combination of the electron-accepting phosphole oxide and the electron-donating diphenylamino group in **1** is, in more than one way, crucial for the presence of the observed outstanding photophysical properties (Table 1; for exhaustive

data, see Table S1 in the Supporting Information). Firstly, a comparison between **1** and **2** shows the importance of the electron-donating properties of the diphenylamino group in **1**. While the absorption spectra of the anisyl derivative **2** showed subtle solvatochromism ($\lambda_{abs} = 359$–367 nm), the emission spectra showed a bathochromic shift with increasing solvent polarity. However, the shift for **2** from toluene to ethanol ($1310\ cm^{-1}$) was measured to be significantly smaller than that in **1** ($2080\ cm^{-1}$). Based on TD-DFT calculations at the PBE0/6-31 + G(d) level of theory, the HOMO of **1** is mostly localized on the electron-donating triphenylamine moiety, whereas that of **2** is delocalized over the 2-anisylbenzophosphole moiety. Accordingly, the character of S_0–S_1 transitions in **1** exhibits the intramolecular charge transfer (ICT) character from the triphenylamine moiety to the electron-accepting benzophosphole oxide moiety, whereas that of **2** is attributable to π–π* transition. The calculated values for the oscillator strengths are 0.396 and 0.265 in **1** and **2**, respectively. The higher value for **1** is consistent with a larger molar extinction coefficient for **1** ($\varepsilon = 1.87 \times 10^4\ M^{-1}\ cm^{-1}$) compared to **2** ($\varepsilon = 1.03 \times 10^4\ M^{-1}\ cm^{-1}$), which should, at least in part, account for the higher quantum yield of **1** relative to **2**.

Secondly, a comparison of **1** with the phosphole sulfide **3** and phosphonium salt **4** illustrates the impact of the electron-accepting character of the benzophosphole moiety. In terms of the LUMO levels, the parent phosphole rings with P=O or P=S moieties should possess a comparable electron-accepting character (see Figure S10 in the Supporting Information). Commensurate with this similarity, **1** and **3** exhibit comparable photophysical properties. For example, **3** shows high fluorescence quantum yields both in polar (DMSO: $\Phi_F = 0.61$) and in protic (EtOH: $\Phi_F = 0.76$) solvents, and the maximum fluorescence emission wavelengths are comparable to those of **1**. In contrast, **4** exhibits, even in toluene, a 33 nm bathochromically shifted absorption maximum, as well as a 144 nm red-shifted fluorescence maximum relative to that of **1** (see Figure S4 in the Supporting Information and Table 1). These large differences are obviously due to the much stronger electron-accepting character of the phosphonium moiety. Irrespective of the solvent polarity, **4** exhibits substantially lower Φ_F values associated with these red-shifted emissions.

Thirdly, a comparison with the thiophene dioxide congener **5** provides insight into the crucial role of the P=O moiety with respect to the strong fluorescence. The parent thiophene dioxide has a lower LUMO level compared to that of phosphole oxide (Figure S10). Whereas **5** exhibits, in nonpolar solvents, a maximum emission wavelength at slightly shorter wavelengths compared to **1**, its maximum emission wavelength in DMSO is bathochromically shifted by 35 nm (see Figure S5 in the Supporting Information). An even more significant difference is observed for the fluorescence quantum yield of **5** in polar or protic solvents, which is much lower than that of **1** (Table 1).

These comparisons clearly demonstrate that the use of a sufficiently strong electron-accepting ring is crucial to preserving intense fluorescence in polar or protic solvents. The fluorescence intensity in such solvents should largely rely on the dynamics of the excited state. Therefore, rate constants for the radiative (k_r) and nonradiative (k_{nr}) decay were determined based on fluorescence quantum yield and lifetime values (τ). While the k_r values in DMSO are comparable for **1**, **4**, and **5** (0.89–$1.1 \times 10^8\ s^{-1}$), the k_{nr} values of **4** and **5** ($52 \times 10^8\ s^{-1}$ and $15 \times 10^8\ s^{-1}$, respectively) are much higher than that of **1** ($0.60 \times 10^8\ s^{-1}$). These results indicate that even though the presence of a strong electron-accepting ring skeleton is crucial for the bathochromically shifted emission, excessive electron-accepting properties may accelerate the nonradiative decay process from the excited singlet state.

Although the photophysical properties of **1** and **3** are almost comparable, their solubility in polar solvents differs greatly. The solubility of phosphole oxide **1** in DMSO ($17.4\ g\,L^{-1}$) is significantly higher than that of phosphole sulfide **3** ($0.8\ g\,L^{-1}$). This difference most probably results from the more polarized P=O moiety relative to the P=S moiety. Electron densities on the P, O, and S atoms in **1** and **3** were calculated by natural population analysis,[16] using the B3LYP hybrid functional in combination with the 6-311G(d) basis set. For the P and O atoms in **1**, electron density values of 1.88 and −1.06, respectively, were calculated, whereas in **3**, values of 1.32 and −0.58 were obtained for the P and S atoms, respectively.

An advantageous feature of **1** for the application as a fluorescent bioimaging probe is the drastic color change of the fluorescence emission as a function of the solvent polarity, that is, the color change from a bluish green in toluene to a reddish orange in DMSO (Figure 2a). Notably, the Lippert–Mataga plot[6] for **1** in various solvents, including the protic solvents ethanol and methanol, showed high linearity ($R^2 = 0.93$; Figure 2b). This linearity suggests that the specific

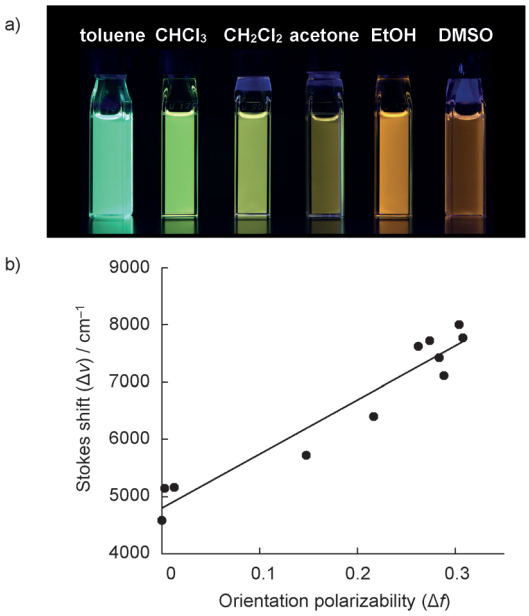

Figure 2. Solvent dependence of the fluorescence of **1**: a) Photos of the color change of the fluorescence emission of **1** in various solvents. b) A Lippert–Mataga plot for **1** in various solvents ($R^2 = 0.93$), whereby $\Delta\nu$ and Δf represent the Stokes shift ($\nu_{abs} - \nu_{em}$) and the orientation polarizability of solvents $(\varepsilon-1)/(2\varepsilon+1) - (n^2-1)/(2n^2+1)$, respectively. ε = dielectric constant, n = refractive index.

solvent effect, resulting from the hydrogen bonding in protic solvents, is not significant despite the presence of the polar P=O moiety. Therefore, a simple monitoring of the emission maxima should allow discrimination of polarity changes/differences in biological media.

To evaluate the utility of **1** as a fluorescent probe for the environmental polarity in biological systems, the dependence of the fluorescence spectra of **1** on the pH value was examined in aqueous solutions. Because of the low solubility of **1** in water, a mixed solvent system, consisting of DMSO and pH-buffered solution (7:3 v/v), was used. The emission spectrum remained unchanged for a wide range of pH values (see Figure S6 in the Supporting Information), thus indicating that the fluorescence properties of **1** are not affected by an intracellular pH change. Subsequently, the photostability of **1** was investigated in ethanol under irradiation with a Xe discharge lamp (300 W), and compared to the performance of other representative dyes, such as BODIPY 493/503, fluorescein, and prodan under the same experimental conditions. The compound **1** was found to be more stable relative to all the reference dyes (see Figure S7 in the Supporting Information). Specifically, **1** showed an absorbance decrease of only about 15% after 30 minutes of irradiation, whereas for example, prodan was subjected to a decrease of more than 60%. Finally, an MTT assay showed that **1** exhibits no cytotoxicity towards HeLa cells at concentrations below 5 μM, which is high enough for cellular staining experiments (see Figure S8 in the Supporting Information).

To demonstrate a practical application of **1**, fluorescence imaging of 3T3-L1 preadipocytes was examined using a confocal microscope equipped with a GaAsP multichannel spectral detector (Figure 3). We expected to be able to visualize the formation of fat in the cells, as the color change of the fluorescence emission should correspond to the polarity change in subcellular compartments during the adipogenic differentiation process. Incubation of 3T3-L1 cells with 1 μM of **1** in Dulbecco's modified Eagle's medium (DMEM) for 2 hours at 37 °C revealed a diffuse staining pattern with several bright spots (0 day; Figure 3a), thus suggesting that **1** should be membrane permeable. The fluorescence spectra of the bright spots (e.g. the spot indicated by the green circle) exhibited an emission maximum between $\lambda = 521$ and 530 nm, whereas the emission spectrum in other intracellular domains (e.g. indicated by the red circle) exhibited emission maxima at a longer wavelength ($\lambda = 556$–565 nm). Using these spectral properties, the image was unmixed into two components shown in green (Figure 3b) and orange (Figure 3c), respectively. The difference in the emission properties clearly demonstrates that **1** allows a discrimination of the environmental polarity in the cells, as the polarity of the former compartment is lower than that of the latter. As the differentiation of 3T3-L1 cells into adipocytes proceeded, lipid droplets increased in both number and size were found in the bright-field images (Figure 3d). The deconvoluted images, using the selected pixels with green color (Figure 3b), strongly support that probe **1** is dissolved in the hydrophobic lipid droplets and thus signals their polarity. In contrast, the emission intensities in the other domains gradually decreased during the adipogenic differentiation (Figure 3c), which may correspond to a concentration decrease of filamentous actin (F-actin).[17] The observed sensitivity of **1** towards environmental polarity, combined with suitable spectral imaging techniques, should allow an elucidation of the molecular mechanisms that control the balance between adipogenesis and osteogenesis in mesenchymal stem cells.[18]

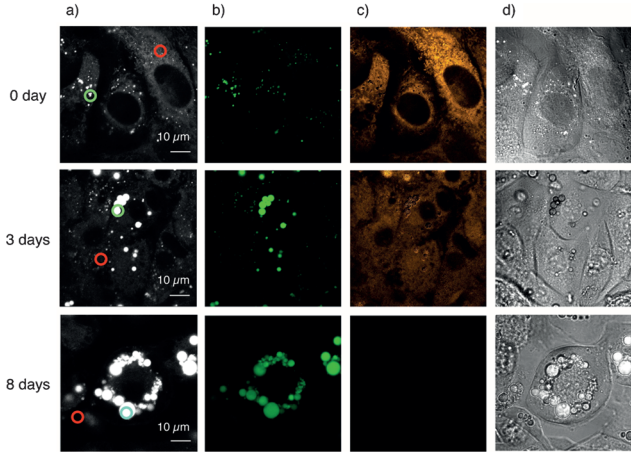

Figure 3. Confocal microphotographs of 3T3 L1 preadipocytes (top) and adipocytes after 3 days (middle) and 8 days (bottom) of differentiation. The cells were stained with **1** for 2 h prior to examination: a) Lambda stack images in the emission range from $\lambda = 416$ to 689 nm with excitation at 405 nm. b, c) Linear-deconvolution images using reference spectra of selected pixels. The exhibited emission maxima in the range of $\lambda = 521$–530 nm (green circle) and $\lambda = 556$–565 nm (red circle), are shown in green and orange, respectively. d) Bright-field images.

In summary, a polarity-sensitive benzophosphole oxide-based fluorophore with a high fluorescence quantum yield was developed. While this benzophosphole oxide with an electron-donating (diphenylamino)phenyl group shows an almost constant absorption around $\lambda_{abs} = 405$ nm, it also exhibits a significant color change of the fluorescence emission as a function of the polarity of the surrounding environment. In addition, the benzophosphole oxide shows a high photostability and no cytotoxicity. Moreover, we demonstrated that this fluorescent probe allows discrimination of the cellular environment in adipocytes based on the fluorescence emission color, which constitutes the first report on staining living animal cells with phosphole-based fluorescence dyes. Future work will be directed towards the enhancement of the water-solubility of these compounds, as well as towards more bathochromically shifted emission colors from further modifications at 3-position and/or from using other benzophosphole skeletons.

Keywords: fluorescent probes · imaging agents · phosphorus heterocycles · phosphole · solvatochromism

How to cite: *Angew. Chem. Int. Ed.* **2015**, *54*, 4539–4543
Angew. Chem. **2015**, *127*, 4622–4626

[1] For recent reviews, see: a) F. Mathey, *Angew. Chem. Int. Ed.* **2003**, *42*, 1578–1604; *Angew. Chem.* **2003**, *115*, 1616–1643; b) M. Hissler, P. W. Dyer, R. Réau, *Coord. Chem. Rev.* **2003**, *244*,

1 – 44; c) T. Baumgartner, R. Réau, *Chem. Rev.* **2006**, *106*, 4681 – 4727; d) J. Crassous, R. Réau, *Dalton Trans.* **2008**, 6865 – 6876; e) Y. Matano, H. Imahori, *Org. Biomol. Chem.* **2009**, *7*, 1258 – 1271; f) Y. Ren, T. Baumgartner, *Dalton Trans.* **2012**, *41*, 7792 – 7800; g) T. Baumgartner, *Acc. Chem. Res.* **2014**, *47*, 1613 – 1622; h) M. Stolar, T. Baumgartner, *Chem. Asian J.* **2014**, *9*, 1212 – 1225.

[2] L. Nyulászi, *Chem. Rev.* **2001**, *101*, 1229 – 1246.

[3] a) C. Fave, T. Y. Cho, M. Hissler, C. W. Chen, T. Y. Luh, C. C. Wu, R. Réau, *J. Am. Chem. Soc.* **2003**, *125*, 9254 – 9255; b) H. C. Su, O. Fadhel, C. J. Yang, T. Y. Cho, C. Fave, M. Hissler, C. C. Wu, R. Réau, *J. Am. Chem. Soc.* **2006**, *128*, 983 – 995; c) O. Fadhel, M. Gras, N. Lemaitre, V. Deborde, M. Hissler, B. Geffroy, R. Réau, *Adv. Mater.* **2009**, *21*, 1261 – 1265; d) D. Joly, D. Tondelier, V. Deborde, B. Geffroy, M. Hissler, R. Réau, *New J. Chem.* **2010**, *34*, 1603 – 1611; e) D. Joly, D. Tondelier, V. Deborde, W. Delaunay, A. Thomas, K. Bhanuprakash, B. Geffroy, M. Hissler, R. Réau, *Adv. Funct. Mater.* **2012**, *22*, 567 – 576; f) H. Chen, W. Delaunay, J. Li, Z. Y. Wang, P. A. Bouit, D. Tondelier, B. Geffroy, F. Mathey, Z. Duan, R. Réau, M. Hissler, *Org. Lett.* **2013**, *15*, 330 – 333; g) H. Tsuji, K. Sato, Y. Sato, E. Nakamura, *J. Mater. Chem.* **2009**, *19*, 3364 – 3366.

[4] a) Y. Matano, T. Miyajima, T. Fukushima, H. Kaji, Y. Kimura, H. Imahori, *Chem. Eur. J.* **2008**, *14*, 8102 – 8115; b) A. Saito, T. Miyajima, M. Nakashima, T. Fukushima, H. Kaji, Y. Matano, H. Imahori, *Chem. Eur. J.* **2009**, *15*, 10000 – 10004; c) Y. Matano, A. Saito, T. Fukushima, Y. Tokudome, F. Suzuki, D. Sakamaki, H. Kaji, A. Ito, K. Tanaka, H. Imahori, *Angew. Chem. Int. Ed.* **2011**, *50*, 8016 – 8020; *Angew. Chem.* **2011**, *123*, 8166 – 8170.

[5] a) A. Kira, Y. Shibano, S. Kang, H. Hayashi, T. Umeyama, Y. Matano, H. Imahori, *Chem. Lett.* **2010**, *39*, 448 – 450; b) Y. Matano, A. Saito, Y. Suzuki, T. Miyajima, S. Akiyama, S. Otsubo, E. Nakamoto, S. Aramaki, H. Imahori, *Chem. Asian J.* **2012**, *7*, 2305 – 2312; c) Y. Matano, H. Ohkubo, Y. Honsho, A. Saito, S. Seki, H. Imahori, *Org. Lett.* **2013**, *15*, 932 – 935; d) Y. Matano, H. Ohkubo, T. Miyata, Y. Watanabe, Y. Hayashi, T. Umeyama, H. Imahori, *Eur. J. Inorg. Chem.* **2014**, 1620 – 1624; e) H. Tsuji, K. Sato, Y. Sato, E. Nakamura, *Chem. Asian J.* **2010**, *5*, 1294 – 1297.

[6] J. R. Lakowicz, *Principles of Fluorescence Spectroscopy*, 3rd ed., Springer, **2006**.

[7] a) L. A. Bagatolli, *Biochim. Biophys. Acta Biomembr.* **2006**, *1758*, 1541 – 1556; b) A. P. Demchenko, Y. Mély, G. Duportail, A. S. Klymchenko, *Biophys. J.* **2009**, *96*, 3461 – 3470; c) A. S. Klymchenko, R. Kreder, *Chem. Biol.* **2014**, *21*, 97 – 113; d) G. S. Loving, M. Sainlos, B. Imperiali, *Trends Biotechnol.* **2010**, *28*, 73 – 83.

[8] a) G. Weber, F. J. Farris, *Biochemistry* **1979**, *18*, 3075 – 3078; b) Y. Niko, S. Kawauchi, G. Konishi, *Chem. Eur. J.* **2013**, *19*, 9760 – 9765.

[9] a) G. Weber, D. J. R. Laurence, *Biochem. J.* **1954**, *56*, xxxi; b) D. C. Turner, L. Brand, *Biochemistry* **1968**, *7*, 3381 – 3390; c) S. H. Hüttenhain, W. Balzer, R. Feldmann, *Z. Naturforsch. A* **1994**, *49*, 1087 – 1090.

[10] Z. Diwu, Y. X. Lu, C. L. Zhang, D. H. Klaubert, R. P. Haugland, *Photochem. Photobiol.* **1997**, *66*, 424 – 431.

[11] a) P. Greenspan, E. P. Mayer, S. D. Fowler, *J. Cell Biol.* **1985**, *100*, 965 – 973; b) J. Jose, K. Burgess, *J. Org. Chem.* **2006**, *71*, 7835 – 7839.

[12] a) T. Sanji, K. Shiraishi, T. Kashiwabara, M. Tanaka, *Org. Lett.* **2008**, *10*, 2689 – 2692; b) H. Tsuji, K. Sato, L. Ilies, Y. Itoh, Y. Sato, E. Nakamura, *Org. Lett.* **2008**, *10*, 2263 – 2265; c) Y. R. Chen, W. L. Duan, *J. Am. Chem. Soc.* **2013**, *135*, 16754 – 16757; d) Y. Unoh, K. Hirano, T. Satoh, M. Miura, *Angew. Chem. Int. Ed.* **2013**, *52*, 12975 – 12979; *Angew. Chem.* **2013**, *125*, 13213 – 13217; e) B. Wu, M. Santra, N. Yoshikai, *Angew. Chem. Int. Ed.* **2014**, *53*, 7543 – 7546; *Angew. Chem.* **2014**, *126*, 7673 – 7676.

[13] A. Fukazawa, Y. Ichihashi, Y. Kosaka, S. Yamaguchi, *Chem. Asian J.* **2009**, *4*, 1729 – 1740.

[14] T. Butters, W. Winter, *Chem. Ber.* **1984**, *117*, 990 – 1002.

[15] L. D. Lavis, R. T. Raines, *ACS Chem. Biol.* **2008**, *3*, 142 – 155.

[16] A. E. Reed, R. B. Weinstock, F. Weinhold, *J. Chem. Phys.* **1985**, *83*, 735 – 746.

[17] H. Sonowal, A. Kumar, J. Bhattacharyya, P. K. Gogoi, B. G. Jaganathan, *J. Biomed. Sci.* **2013**, *20*, 71 – 80.

[18] M. Kawai, C. J. Rosen, *Nat. Rev. Endocrinol.* **2010**, *6*, 629 – 636.

Received: January 10, 2015
Published online: March 4, 2015

